Design and Optimization of a Multiband Extra Wideband Ring Patch Antenna for 5G mm-Wave Communication at 28/60/80 GHz Using MLPNN based K-fold cross validation method

Lahcen SELLAK[1,⋆], *Asma* KHABBA[2], *Jamal* Amadid[3], *Samira* CHABAA[1,2], *Saida* IBNYAICH[2], and *Abdelouhab* ZEROUAL[2]

[1] *LISAD Research Laboratory, Industrial Engineering Department, National School of Applied Sciences, Ibn Zohr University, Agadir, Morocco*
[2] *I2SP Research Team, Department of physics, Faculty of Sciences Semlalia, Cadi Ayyad University, Marrakech, Morocco*
[3] *Electronics Department, Higher Institute of Engineering and Business (ISGA), Marrakesh, Morocco*

Abstract. In this paper, we present the design of an innovative Ultra-Wideband (UWB) ring patch antenna customized for 28 GHz, 60 GHz and 80 GHz and 5G mm-Wave communication. The antenna features a ring patch with an embedded small rectangular patch and a partial ground plane. To optimize the antenna dimensions for resonance at 28 GHz, 60 GHz, and 80 GHz, a Multilayer Perceptron Neural Network (MLPNN) was employed with a k-fold cross-validation technique. Simulation results demonstrate that the MLPNN-optimized antenna achieves superior performance metrics, including a low reflection coefficient, efficient radiation patterns, and a wide bandwidth of 13.2 GHz at 28 GHz and an extended bandwidth of 53 GHz spanning from 47 GHz to 100 GHz. These characteristics highlight its potential as a robust solution for next-generation 5G communication systems.
keywords: UWB Ring Patch Antenna, 5G, mm-Wave Communication, RBFNN, Cross Validation.

1 Introduction

The advent of 5G technology promises significant enhancements in wireless communication, particularly through the use of millimeter-wave (mm-Wave) frequencies such as the 28 GHz band [1]. These higher frequencies enable greater bandwidth and faster data rates, essential for supporting the ever-increasing demand for mobile data. However, designing antennas that operate efficiently at these frequencies presents several challenges, including maintaining a compact size, achieving wide bandwidth, and ensuring high gain and efficiency [2]. Traditional antenna designs often fall short of meeting these stringent requirements due to limitations in their structure and optimization techniques. Common issues include narrow bandwidth, suboptimal gain, and inefficient radiation patterns. Furthermore, the increased complexity at higher frequencies necessitates advanced design methodologies to achieve the desired performance [3] .

The integration of machine learning techniques in antenna design has shown promising results in addressing these challenges. Machine learning models, particularly neural networks, have the ability to learn complex patterns and optimize design parameters efficiently. In this context, Multilayer Perceptron Neural Networks (MLPNN) have emerged as a powerful tool for predictive modeling and optimization [4].

Several studies have explored the design of patch antennas operating at 28 GHz. For example, Reference [5] focuses on a microstrip patch antenna optimized for mobile applications, employing FR-4 substrate. The antenna demonstrates favorable impedance features with a return loss of -24.507 dB and VSWR of 1.126, achieving a gain of 7.19 dBi and a bandwidth of 1.352 GHz. However, the elevated loss tangent of FR-4 substrate could potentially affect the antenna's efficiency and performance, particularly at higher millimeter-wave frequencies like 28 GHz. Reference [6] explores microstrip antennas operating at 28 GHz for 5G applications, featuring three models with slot variations to enhance bandwidth and reduce effective area. The use of low-cost FR4 substrate with a dielectric constant of 4.4 and a loss tangent of 0.02 enables compact antenna sizes ($7 \times 7\ mm^2$) with improved bandwidth. However, while slot configurations enhance performance metrics like bandwidth, the trade-off may involve increased complexity in design and fabrication. Reference [7] introduces a dual-band antenna for vehicle-to-vehicle communication, combining a 28 GHz inset-fed rectangular patch with a 5.9 GHz patch antenna. This design achieves a large frequency ratio of 4.74:1, operating across dedicated short-range communications (DSRC) and 5G millimeter-wave bands. It offers a high peak gain of 7.7 dBi in DSRC and 6.38 dBi in the 5G mm-wave band. However, achieving dual-band operation introduces complexity in antenna

⋆e-mail: lahcensellak17@gmail.com

design and fabrication, potentially increasing manufacturing costs and complexity.

In this work, an innovative Ultra-Wideband (UWB) ring patch antenna design is introduced. The antenna comprises a ring patch with a small rectangular patch inserted inside and a partial ground plane. This design aims to achieve resonance at 28 GHz, 60 GHz and 80 GHz, providing a solution to the common limitations of traditional antenna designs.

To accurately predict the optimal dimensions of this antenna, a MLPNN in conjunction with a k-fold cross-validation method is utilized. This approach ensures robust and precise optimization, leading to superior antenna performance suitable for 5G mm-Wave communication. The problem addressed in this paper is the difficulty in achieving a compact, high-performance antenna design for 28 GHz 5G applications using conventional methods. By leveraging advanced machine learning techniques, these limitations are overcome, demonstrating a significant improvement in antenna performance.

After this introduction, the paper is organized as follows: Section 2 describes the proposed antenna layout, detailing the structure and design considerations of the UWB ring patch antenna. Section 3 outlines the proposed method, focusing on the optimization process using the MLPNN approach with k-fold cross-validation. Section 4 delves into the development of the MLPNN model, explaining its architecture, training process, and validation techniques. Section 5 presents the results and discussion, analyzing the simulated performance metrics of the antenna, including reflection coefficient, VSWR, gain, and efficiency, using HFSS and CST software. Finally, Section 6 concludes the paper.

2 Proposed antenna layout

The proposed antenna design features a unique geometry tailored to achieve optimal performance at 28 GHz for 5G mm-Wave applications. The antenna comprises a ring patch with inner radius of R_2 outer radius of R_1 with an embedded small rectangular patch with dimensions of $W_p \times L_p$ centrally located within the ring. This inner rectangular patch serves to enhance the antenna's resonant characteristics and improve impedance matching. The ring patch is meticulously designed to enhance the antenna's UWB performance by supporting a broad bandwidth. It is fed by a microstrip line with dimensions $L_f \times W_f$, while a small rectangular patch, strategically placed at the center of the ring, is fed through a microstrip line with dimensions $L_s \times W_s$. The substrate material used for the antenna is Rogers RT, which has a relative permittivity of 2.2 and a thickness of 0.508 mm an total size of $W_{sub} \times L_{sub}$. This low-loss dielectric material is chosen to minimize signal attenuation and ensure high efficiency. A partial ground plane with dimensions of $W_{sub} \times L_g$ is employed on the opposite side of the substrate, which helps in achieving the desired radiation pattern and further enhances the bandwidth. The dimensions of the ring patch, rectangular patch, and partial ground plane are predicted using the MLPNN based k-fold cross-validation method. This ensures that the antenna operates efficiently at the target frequencies of 28 GHz, 60 GHz and 80 GHz providing robust performance for 5G communication systems.

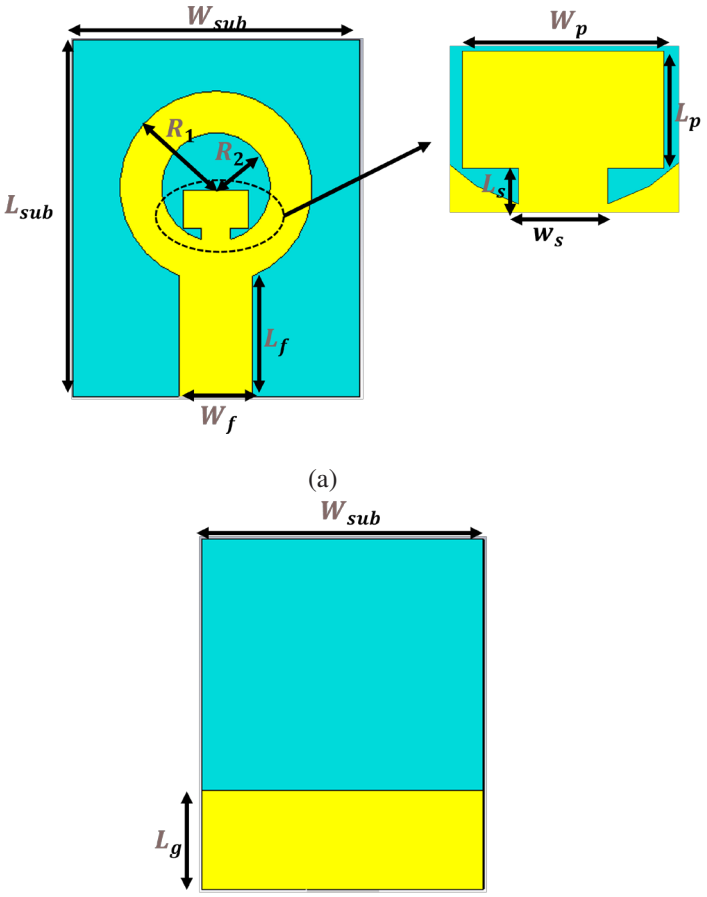

Figure 1. Layout of the proposed antenna: (a) front view, (b) Back view

3 Proposed method

The design and optimization of the proposed UWB ring patch antenna were achieved using a MLPNN model, enhanced by k-fold cross-validation for precise dimension prediction. The proposed method is outlined in Figure 2. The process began with the collection of a comprehensive dataset of antenna dimensions and corresponding performance metrics through extensive simulations. The MLPNN architecture comprised three layers: an input layer, one or more hidden layers with perceptron neurons, and an output layer, with the number of neurons in the hidden layers determined by the problem's complexity and dataset size. The network was trained using optimization techniques to minimize the error between predicted and actual performance metrics. To ensure robustness, k-fold cross-validation was employed, dividing the dataset into k equal-sized folds. Each fold was used once as a validation set while the remaining k-1 folds were used for training. This process was repeated k times, and perfor-

mance metrics were averaged to provide a comprehensive assessment. The final MLPNN model, selected based on cross-validation results, was used to predict the optimal dimensions for achieving resonance at 28 GHz, 60 GHz and 80 GHz. This combined approach ensures the antenna design meets the stringent performance requirements for 5G mm-Wave communication.

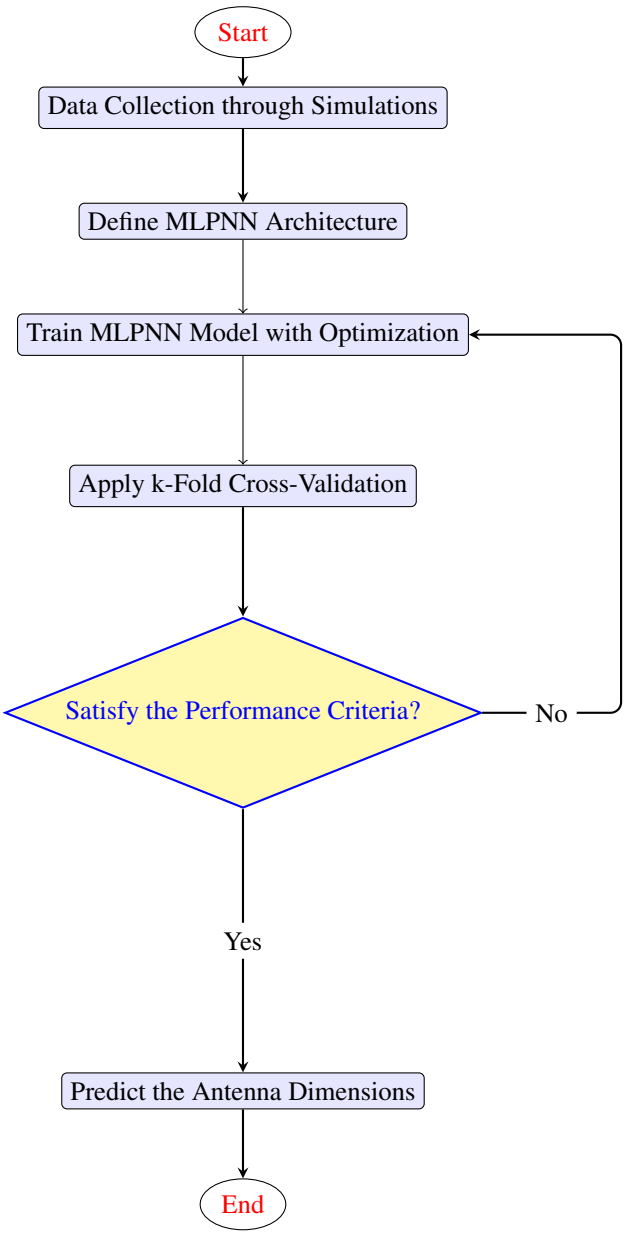

Figure 2. Flowchart of the Proposed Method

4 Developed MLPNN model

The developed MLPNN model is tailored to optimize the dimensions of the UWB ring patch antenna specifically for 28 GHz, 60 GHz and 80 GHz for 5G mm-Wave communication. The model, depicted in Figure 3, takes as inputs the desired resonant frequencies (f_{r_1}, f_{r_2} and f_{r_3}), the height of the substrate (H) and the relative permitivity of the substrate ϵ_r. Using these inputs, the MLPNN predicts the optimal antenna dimensions, which include the patch length (L_p), patch width (W_p), ground plane length (L_g), length of the feed line of the small rectangular patch (L_s), and its width (W_s), inner ring radius (R_1), and outer ring radius (R_2). The architecture of the MLPNN consists of an input layer, one or more hidden layers with perceptron neurons, and an output layer. This configuration allows the model to effectively capture the complex relationships between the input parameters and the antenna's performance metrics, ensuring an optimal design for 5G mm-Wave communication.

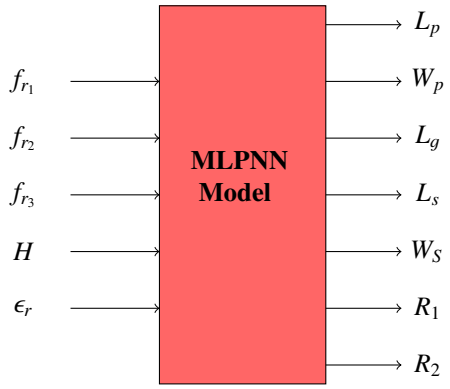

Figure 3. MLPNN model's structure

To develop the MLPNN model, we undertook several methodical steps. Firstly, we created a comprehensive database by systematically varying the antenna parameters and substrate permittivity (ε_r). The corresponding resonance frequencies were recorded. This dataset was gathered using a Visual Basic (VB) script, which enabled MATLAB to control the HFSS simulator. This process resulted in a dataset comprising 599 simulations, each with different antenna dimensions and dielectric substrate characteristics.

Next, we determined the optimal number of hidden layers and neurons in each hidden layer by evaluating various statistical criteria, such as mean squared error (MSE), root mean square error (RMSE) and mean absolute error (MAE). For our model, we chose an architecture with two hidden layers, each containing 25 neurons. We then evaluated several training algorithms, including resilient backpropagation (RP), Polak-Ribiere conjugate gradient (CGP), one-step secant (OSS), scaled conjugate gradient (SCG), and Levenberg-Marquardt (LM). The LM algorithm was found to provide the highest accuracy and was thus selected for training the MLPNN model. The specific parameters and configurations of the MLPNN model are detailed in Table 1.

Table 1. Final configuration of the MLP model

Parameter	Attributes
Number of samples	599
Training algorithm	Levenberg–Marquardt (LM)
Transfer function	Tansig
Network structure	5-25-25-7

After establishing the structure of the MLP model, the efficiency of the model is enhanced using the k-fold cross-validation technique. For this study, a 10-fold cross-validation approach is applied during the training phase. This involves dividing the dataset into 10 equal subsets. Each subset is used as a test set once, while the remaining nine subsets are used for training. This process is repeated 10 times, ensuring that each subset serves as the test set once and as part of the training set nine times. This method allows for comprehensive evaluation and training of the model, leading to improved generalization and robustness. The 10-fold cross-validation procedure is depicted in Figure 4.

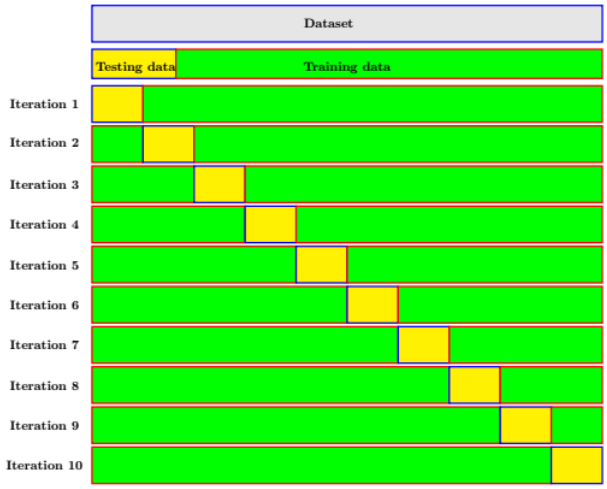

Figure 4. Example of dataset divided using the 10-fold cross-validation method

For every fold, we calculated various statistical metrics, which are detailed in Table 2. The averaged metrics across the folds are: Mean MSE of 0.0441, Mean MAE of 0.1356, and Mean RMSE of 0.2082. These metrics values demonstrate the overall efficacy of the MLP model, with lower values indicating better predictive accuracy and reliability.

Table 2. Errors for each iteration

Iteration	MSE	$MAPE$	$RMSE$
1	0.0498	0.1482	0.2232
2	0.0657	0.1551	0.2563
3	0.0395	0.1421	0.1986
4	0.0212	0.1021	0.1457
5	0.0476	0.1483	0.2181
6	0.0446	0.1401	0.2112
7	0.0468	0.1343	0.2164
8	0.0419	0.1226	0.2047
9	0.0517	0.1470	0.2274
10	0.0324	0.1162	0.1799

The developed MLPNN model was used to predict the optimal dimensions of the UWB ring patch antenna to achieve resonance at 28 GHz, 60 GHz and 80 GHz. These predicted dimensions are presented in Table 3.

Table 3. Predicted dimensions of the proposed antenna

Parameter	L_p	W_p	L_g	L_s
Value (mm)	0.5502	0.9385	1.4561	0.5939
Parameter	W_s	R_1	R_2	
Value (mm)	0.4156	0.7829	1.3833	

5 Results and discussion

This section presents and discusses the simulated results of the proposed UWB ring patch antenna, obtained using HFSS simulation software. Key performance metrics, including the reflection coefficient, Voltage Standing Wave Ratio (VSWR), gain, and efficiency, are evaluated to validate the effectiveness of the antenna design for 5G mm-Wave communication.

The reflection coefficient, also known as the S_{11} parameter, indicates the amount of power reflected back from the antenna. As shown in Figure 5(a), simulations from HFSS demonstrate that the designed antenna achieves a reflection coefficient below the practical threshold of -10 dB across a wide frequency range from 20 to 120 GHz. The antenna is specifically targeted to resonate at three distinct frequencies: 28 GHz, 60 GHz, and 80 GHz. At the desired resonance frequency of 28 GHz, the S_{11} is less than -25 dB, indicating excellent impedance matching. Similarly, the antenna shows significant resonance dips at 60 GHz and 80 GHz of -30 dB and -40 dB, respectively, confirming efficient signal transmission and minimal power loss at these targeted frequencies. In terms of bandwidth, the antenna shows a wide operating range, which is a crucial characteristic for UWB applications. As shown in Figure 5(a), simulations from HFSS show that the designed antenna achieves a reflection coefficient well below the practical threshold of -10 dB across the frequency band spanning from 21.8 to 35 GHz for the first band, indicating a UWB characteristic of 13.2 GHz. For the second band, which contains two resonance frequencies at 60 GHz and 80 GHz, the antenna has a bandwidth of 53 GHz spanning from 47 GHz to 120 GHz. The broad bandwidth ensures that the antenna can support a variety of frequency channels and applications, making it highly versatile for 5G mm-Wave communication. This impedance matching and wideband characteristic can be further validated by the VSWR plot presented in Figure 5(b). As shown, the VSWR value remains between 1 and 2 across the entire working bandwidth, with notable dips at the three targeted resonance frequencies (28 GHz, 60 GHz, and 80 GHz). These dips in VSWR correspond to the resonance frequencies where the antenna achieves optimal performance, confirming efficient power transmission and minimal reflection within the operating frequency range.

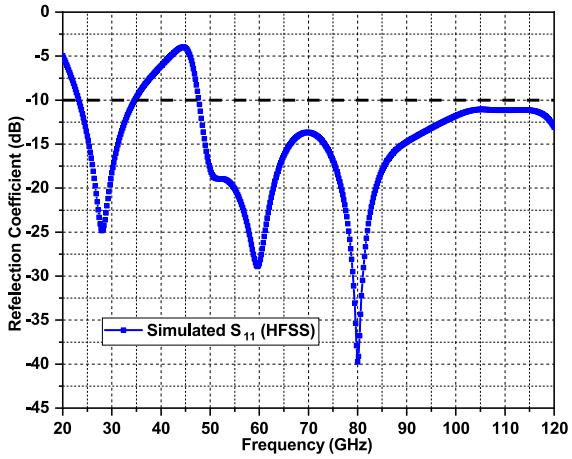

(a)

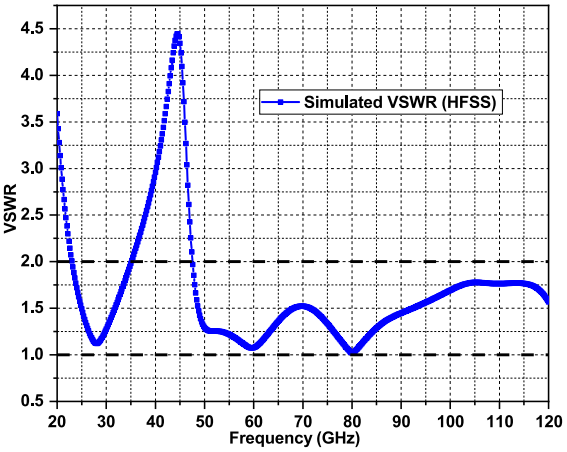

(b)

Figure 5. Characteristics of the suggested antenna: (a) Reflection coefficient, (b) VSWR

To further evaluate the performance of the proposed antenna, Figure 6 presents the radiation patterns of the suggested antenna at the three targeted resonance frequencies: 28 GHz, 60 GHz, and 80 GHz, showcasing both co-polarization (co-pol) and cross-polarization (cross-pol) components for both the E-plane and H-plane. At 28 GHz (Figure 6(a)), the E-plane co-polarization pattern exhibits a bidirectional radiation pattern, indicating strong radiation in two opposite directions, while the cross-polarization pattern shows minimal omnidirectional radiation, suggesting that undesired polarization is uniformly distributed. In the H-plane, the co-polarization pattern is omnidirectional, indicating uniform radiation in all directions, and the cross-polarization pattern is bidirectional with small values, confirming well-controlled cross-polarized radiation. At 60 GHz (Figure 6(b)), the E-plane co-polarization pattern remains bidirectional, with the cross-polarization pattern staying minimal and uniformly distributed. The H-plane co-polarization pattern is omnidirectional, and the cross-polarization pattern continues to exhibit low values, maintaining high polarization purity. At 80 GHz (Figure 6(c)), the E-plane co-polarization pattern maintains its bidirectional nature, with minimal and uniformly distributed cross-polarization. The H-plane co-polarization pattern remains omnidirectional, and the cross-polarization pattern is bidirectional with small values. These radiation patterns across all targeted frequencies validate the antenna's ability to maintain high polarization purity and directivity, making it suitable for 5G mm-Wave communication applications.

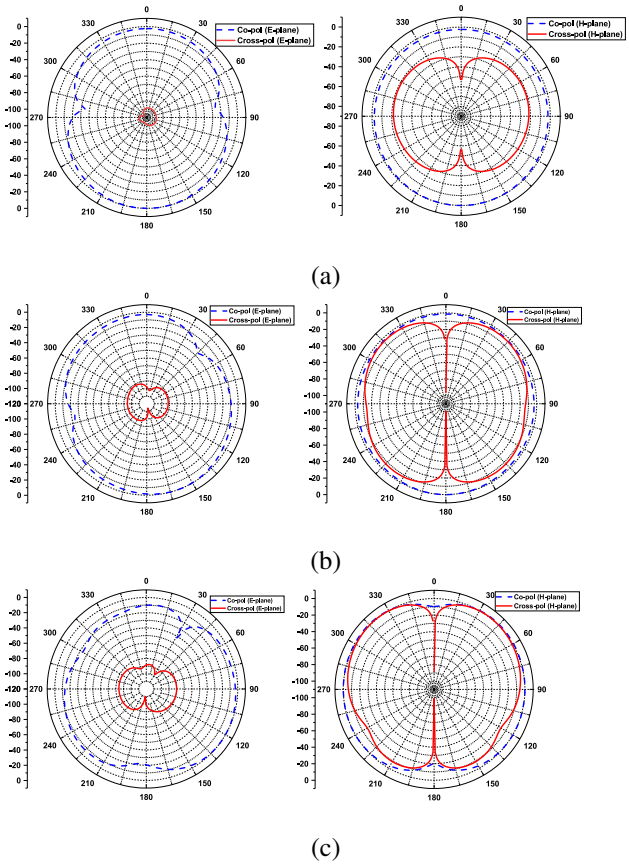

(a)

(b)

(c)

Figure 6. Radiation pattern of the suggested antenna for both E-plane and H-plane at: (a) 28 GHz, (b) 60 GHz, (c) 80 GHz

The figure 7 illustrates the gain and radiation efficiency of the proposed UWB ring patch antenna across a frequency range of 20 to 120 GHz. The gain, depicted by the solid blue line, shows notable peaks at the target resonance frequencies of 28 GHz, 60 GHz, and 80 GHz, indicating efficient radiation at these bands. The highest gain achieved is approximately 5 dB. The dashed red line represents the radiation efficiency, which remains consistently high, above 98.6% throughout the entire frequency range. The efficiency peaks at around 99.8%, confirming the antenna's ability to effectively convert input power into radiated energy with minimal losses, making it suitable for high-performance 5G mm-Wave communication applications.

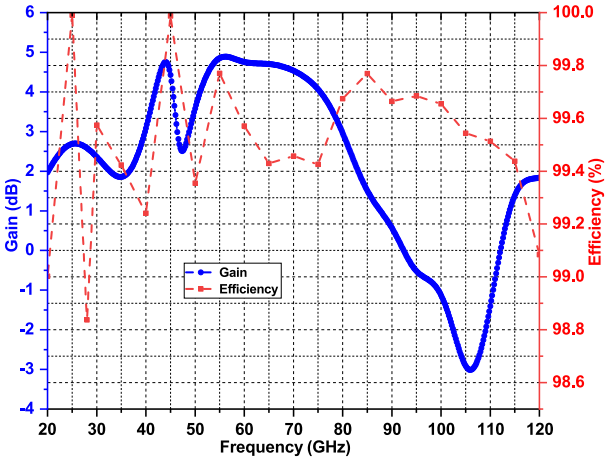

Figure 7. Gain and radiation efficiency vs frequency

Table 4 presents a comparative analysis of various UWB patch antennas documented in the literature. The proposed antenna operates at multiple frequencies, including 28 GHz, 60 GHz, and 80 GHz, and is notably compact with dimensions of 4.11×5.13 mm^2. It achieves a substantial bandwidth of 13.2 GHz at 28 GHz and an extended bandwidth of 53 GHz spanning from 47 GHz to 120 GHz in HFSS, which outperforms other antennas in the comparison. Moreover, the proposed antenna's maximum gain of 5 dB and impressive efficiency of 99% are significant advantages. In comparison, the design in [6] with a size of 7×7 mm^2 has a bandwidth of 2.62 GHz and a gain of 6.59 dB but lacks efficiency data. Our proposed antenna surpasses this with a much wider bandwidth (13.2 GHz and 53 GHz) and higher efficiency (99%). The design in [7], measuring 22×26 mm^2, offers a bandwidth of 4.5 GHz with gains around 5.8 dB and efficiencies reaching 98%. Our antenna is more compact and offers a significantly wider bandwidth. Similarly, [8], with dimensions of 5×3 mm^2, provides a bandwidth of 4.41 GHz, gains near 4.49 dB, and efficiencies of 89%. Our antenna provides greater bandwidth and higher efficiency. Additionally, [9] offers a moderate bandwidth of 5 GHz and varying gains but lacks efficiency data, whereas our antenna offers more than ten times the bandwidth and has documented high efficiency. Furthermore, [10], measuring 40×40 mm^2, achieves substantial bandwidths of 17 GHz but lacks data on gain and efficiency. Our proposed antenna is much more compact and provides a comparable wide bandwidth. The design in [11] offers a bandwidth of 15 GHz with gains of 5.2 dB and efficiency of 98%. Our antenna has a comparable gain, higher efficiency, and a broader bandwidth. Likewise, [12] with a bandwidth of 9.52 GHz, gains of 3.5 dB, and efficiency of 97%, is surpassed by our proposed antenna in both bandwidth and efficiency. Moreover, [13] achieves a bandwidth of 10 GHz with gains around 5.9 dB and efficiencies of 98.7%. Our proposed antenna provides a broader bandwidth and slightly higher efficiency. Lastly, the designs in [14] operating at 60/80/100 GHz with sizes around 5.12×8 mm^2 achieve gains of 5.7 dB and efficiencies of 70%. Our proposed antenna offers better efficiency and comparable gain while being more compact. This comparison highlights the proposed antenna's superior performance in terms of bandwidth, compact size, and efficiency, showcasing the trade-offs between size, bandwidth, gain, and efficiency across different implementations for 5G mm-Wave communication applications.

Table 4. Comparison of the proposed UWB patch antenna single element with the relevant researchers

Ref.	Fr (GHz)	Size(mm^2)	BW (GHz)	Max. Gain (dB)	Eff. (%)
[6]	28	7×7	2.62	6.59	NA
[7]	28	22×26	4.5	5.8	98
[8]	28	5×3	4.41	4.49	89
[9]	28	8.4×6.2	5	5.06	-
[15]	28	14×14	2	NA	NA
[10]	28	40×40	17	NA	NA
[11]	28	12×10	15	5.2	98
[12]	28	12×10	9.52	3.5	97
[16]	28	9.5×7.7	1.2	NA	NA
[13]	28	11×8	10	5.9	98.7
[17]	28/38	27.65×12	4.3/3.8	NA	NA
[14]	60/80/100	5.12×8	60 GHz	5.7	70
This work	28/60/80	4.11×5.13	13.2/53	5	99

6 Conclusion

This study has demonstrated the successful design and optimization of a UWB ring patch antenna for 28, 60 GHz, and 80 GHz for 5G mm-Wave communication using a MLPNN. The antenna, featuring a novel structure with a ring patch and an embedded rectangular patch, was meticulously optimized to achieve resonance at 28 GHz, 60 GHz, and 80 GHz. By employing MLPNN with k-fold cross-validation, we ensured accurate dimension prediction and superior antenna performance. Simulation results confirmed the antenna's excellent characteristics, including a low reflection coefficient, efficient radiation patterns, and a wide bandwidth of 13.2 GHz at 28 GHz and an extended bandwidth of 53 GHz spanning from 47 GHz to 100 GHz. These features are crucial for meeting the demanding requirements of 5G applications. The findings underscore the efficacy of machine learning techniques in advancing antenna design, paving the way for enhanced performance and reliability in future 5G communication systems.

References

[1] W. Hong, Z.H. Jiang, C. Yu, D. Hou, H. Wang, C. Guo, Y. Hu, L. Kuai, Y. Yu, Z. Jiang et al., IEEE Journal of Microwaves **1**, 101 (2021)

[2] S. Tripathi, N.V. Sabu, A.K. Gupta, H.S. Dhillon, in *6G Mobile Wireless Networks* (Springer, 2021), pp. 83–121

[3] N. Rajatheva, I. Atzeni, E. Bjornson, A. Bourdoux, S. Buzzi, J.B. Dore, S. Erkucuk, M. Fuentes, K. Guan, Y. Hu et al., arXiv preprint arXiv:2004.14247 (2020)

[4] H.M. El Misilmani, T. Naous, S.K. Al Khatib, International Journal of RF and Microwave Computer-Aided Engineering **30**, e22356 (2020)

[5] M.S. Rana, M. Moniruzzaman, A.N. Biswas, T. Azad, S. Mondal, A.T.U. Islam, S. Pal, R. Islam, M.R. Islam, S. Hossain et al., Indonesian Journal of Electrical Engineering and Informatics (IJEEI) **11**, 967 (2023)

[6] P. Merlin Teresa, G. Umamaheswari, IETE Journal of Research **68**, 3778 (2022), publisher: Taylor & Francis _eprint: https://doi.org/10.1080/03772063.2020.1779620

[7] S.R. Govindarajulu, M.N.A. Tarek, M.R. Guerra, A. Hassan, E. Alwan, Sensors **23**, 6108 (2023)

[8] P. Kumar, T. Ali, O.P. Kumar, S. Vincent, P. Kumar, Y. Nanjappa, S. Pathan, Micromachines **14**, 5 (2023), number: 1 Publisher: Multidisciplinary Digital Publishing Institute

[9] R. Przesmycki, M. Bugaj, L. Nowosielski, Electronics **10**, 1 (2021), number: 1 Publisher: Multidisciplinary Digital Publishing Institute

[10] D.A. Sehrai, M. Abdullah, A. Altaf, S.H. Kiani, F. Muhammad, M. Tufail, M. Irfan, A. Glowacz, S. Rahman, Electronics **9** (2020)

[11] M.A. Khan, A.G. Al Harbi, S.H. Kiani, A.N. Nordin, M.E. Munir, S.I. Saeed, J. Iqbal, E.M. Ali, M. Alibakhshikenari, M. Dalarsson, Applied Sciences **12** (2022)

[12] M.I. Khan, S. Khan, S.H. Kiani, N. Ojaroudi Parchin, K. Mahmood, U. Rafique, M.M. Qadir, Electronics **11** (2022)

[13] A. Khabba, J. Amadid, S. Mohapatra, Z. El Ouadi, S. Ahmad, S. Ibnyaich, A. Zeroual, Applied Physics A **128**, 725 (2022)

[14] H.A. Rahman, M.M. Khan, M. Baz, M. Masud, M.A. AlZain, International Journal of Antennas and Propagation **2021**, 8725263 (2021)

[15] M.M. Kamal, S. Yang, X.c. Ren, A. Altaf, S.H. Kiani, M.R. Anjum, A. Iqbal, M. Asif, S.I. Saeed, Electronics **10** (2021)

[16] S. Tariq, S.I. Naqvi, N. Hussain, Y. Amin, IEEE Access **9**, 51805 (2021)

[17] A.R. Sabek, W.A. Ali, A.A. Ibrahim, Journal of Infrared, Millimeter, and Terahertz Waves **43**, 335 (2022)